Journal of Sound and Vibration (1999) **224**(5), 941–951
Article No. jsvi.1998.2144, available online at http://www.idealibrary.com on IDEAL®

DYNAMIC ANALYSIS OF FOUNDATION PLATES USING A CONSISTENT VLASOV MODEL

A. Daloğlu, A. Doğangün and Y. Ayvaz
Department of Civil Engineering, Karadeniz Technical University,
61080 *Trabzon, Turkey*

(*Received* 8 *April* 1998, *and in final form* 26 *November* 1998)

1. INTRODUCTION

Plates supported by elastic foundations present very common technical problems in structural and geotechnical engineering. The majority of research work in this area has been done using the classical Winkler model [1] where a coefficient k called the subgrade reaction of the foundation is employed [2]. Many other models have been used but the Winkler model is often adapted [3] because of its simplicity. The problems of vibrations and stability of beams on elastic foundations by using a Winkler model are solved by several researchers such as Clastornik *et al*. [4], Eisenberger *et al*. [5], Eisenberger and Clastornik [6], De Rosa [7] and Ding [3]. Recognizing the behavioural inconsistency of the Winkler model, many researchers attempted to make the model more realistic by providing some interaction among the Winkler springs, and introducing a two parameter foundation model. Despite their simplicity, two parameter foundation models failed to gain acceptance in the engineering community [8] because of their lack of consistency. Dynamic analysis of beams resting on elastic foundations using two parameter models have been performed by Franciosi and Masi [9], De Rosa [10] and Yokoyama [11]. Vlasov and Leont'ev [12] introduced an improved model by introducing a third parameter, γ, to represent the distribution of the displacements in the vertical direction. This Vlasov model is applied to the dynamic analysis of beams on elastic foundations by Ayvaz and Daloğolu [13] and Daloğlu and Ayvaz [14]. But no references have been found for the application of a consistent Vlasov model to dynamic analysis of plates resting on elastic foundations subjected to external loads.

The authors have developed a mathematical model for the dynamic analysis of rectangular plates on elastic foundations using three parameters such as k, t, and γ. A computer program is coded in FORTRAN for the dynamic out-of-plane response of plates resting on elastic foundations. Rectangular finite elements are used to model the plate–soil system and the Newmark-β method is used for time integration. The computational technique is an iterative process which is dependent upon the γ parameter. A number of graphs are presented to show the effects of the subsoil depth, plate dimensions, and their ratios on the dynamic response of rectangular plates on elastic foundations subjected to both uniformly distributed load and concentrated load at the center of the plates.

0022–460X/99/300941 + 11 $30.00/0

2. MATHEMATICAL MODEL

The dynamics of elastic structures based on Hamilton's variational principle is

$$\delta \int_{t_1}^{t_2} \Pi \, \mathrm{d}t = 0, \tag{1a}$$

where

$$\Pi = \Pi_k - \Pi_{ie}, \tag{1b}$$

in which Π_k is the kinetic energy which can be expressed as

$$\Pi_k = \tfrac{1}{2} \int_\Omega \dot{\mathbf{w}} \boldsymbol{\mu} \dot{\mathbf{w}} \, \mathrm{d}\Omega, \tag{2a}$$

where $\mathbf{w}$ represents the vector of generalized displacement components relevant to inertial forces, the dot denotes the partial derivative with respect to the time variable, t, $\boldsymbol{\mu}$ is the mass density matrix, Ω is the domain of the plate. The integration is performed in an arbitrary time interval $t_1 \leqslant t \leqslant t_2$. Π_{ie} are the potential energies of internal and external forces and can be written as

$$\Pi_{ie} = \tfrac{1}{2} \int_\Omega \boldsymbol{\varepsilon}^{\mathrm{T}} \boldsymbol{\sigma} \, \mathrm{d}\Omega - \int_\Omega q \mathbf{w} \, \mathrm{d}\Omega \tag{2b}$$

where $\boldsymbol{\varepsilon}$ and $\boldsymbol{\sigma}$ are strain and stress tensors, q is applied distributed load. The displacement function, $\mathbf{w}$, can be expressed as

$$\mathbf{w} = \mathbf{N}\mathbf{W}, \tag{2c}$$

in which $\mathbf{N}$ can be defined by shape functions in natural co-ordinates and $\mathbf{W}$ is the vector of deformation parameters. Then equation (1b) in expanded form may be written as [15],

$$\Pi = \tfrac{1}{2} \dot{\mathbf{W}} \mathbf{M} \dot{\mathbf{W}} - \tfrac{1}{2} \mathbf{W}^{\mathrm{T}} \mathbf{K} \mathbf{W} + \mathbf{W}^{\mathrm{T}} \mathbf{F}, \tag{2d}$$

in which $\mathbf{K}$ represents the stiffness matrix of the soil–structure system and $\mathbf{F}$ is the load vector. By substituting equation (2d) into equation (1a) and applying the variational principle, the following expression may be obtained

$$\int_{t_1}^{t_2} \delta \mathbf{W} (-\mathbf{M} \ddot{\mathbf{W}} - \mathbf{K}\mathbf{W} + \mathbf{F}) \, \mathrm{d}t = 0. \tag{2e}$$

Finally, the dynamic equilibrium condition including inertial forces according to the d'Alembert principle is

$$\mathbf{K}\mathbf{W} + \mathbf{M} \ddot{\mathbf{W}} = \mathbf{F}. \tag{2f}$$

See reference [16] for an evaluation of the stiffness and mass matrices. Equivalent nodal loads $\mathbf{F}$ in equation (2f) can be evaluated as

$$\mathbf{F} = \int_\Omega \mathbf{N}^{\mathrm{T}} q \, \mathrm{d}\Omega. \tag{3}$$

Boundary conditions to consider the effect of the infinite soil domain outside the plate need to be evaluated to solve the equation system. See references [15, 17] for details.

It should be noted that, in this study, the Newmark-β method is used for the time integration of equation (2f) by using the average acceleration method [18], and that the computational technique used to get the displacements of the plates considered is the same as used in reference [16].

3. NUMERICAL EXAMPLES

3.1. *Data for numerical examples*

In the light of the results given in references [8, 13] the depths, H, of the subsoil (see Figure 1) used are 5, 10 and 15 m. The aspect ratios, ly/lx, of the plate used are 1, 1·5 and 2·0. The ratios H/ly used are 0·25, 0·50, 0·75 and 1·0 for each subsoil depth considered. The shorter length of the plate, lx, is kept constant at 10 m. The mass densities of the plate and the subsoil are taken to be 2500 kg/m^3 and 1700 kg/m^3, respectively, for the calculation of the mass matrix.

In order to obtain the response of each plate, a uniformly distributed load (UDL) of -30 kN/m^2 and a concentrated load (CL) of -1000 kN at the center of the plate, are used.

For the sake of accuracy in the results, rather than starting with a set of values for the finite element mesh size and time increment, the mesh size and the time increment required to produce the desired accuracy are determined. This analysis is undertaken separately for the mesh size and time increment. To find out the required finite element mesh size, the time increment is fixed, and the convergence of the maximum displacement is checked for different mesh sizes. To obtain the required time increment, the finite element mesh size is fixed, and the convergence of the maximum displacement is checked for different time

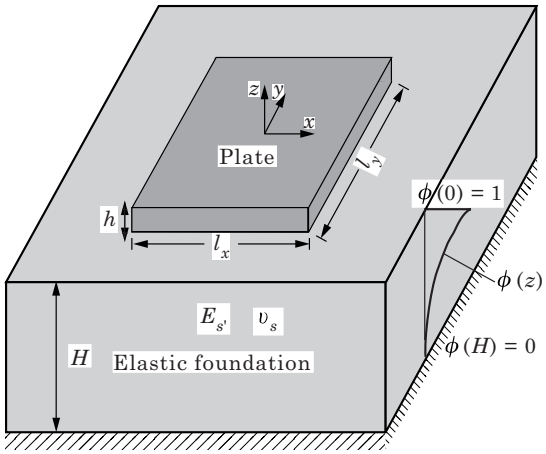

Figure 1. A sample plate resting on an elastic foundation.

increments. In conclusion, the results have an acceptable error when using equally spaced 10 × 10 elements for a 10 m × 10 m plate for the uniformly distributed load if a 0·01 s time increment is used, and when using unequally spaced 10 × 10 elements for a 10 m × 10 m plate for the concentrated load if a 0·001 s time increment is used.

3.2. *Results*

The purpose of this study is to present the time histories of the displacements at different points on the plates for different subsoil depths and aspect ratios, but presentation of all of the time histories would take up excessive space. Therefore, only the maximum displacement for different aspect ratios and subsoil depths are presented after several time histories are given. This simplification to the presentation of the maximum responses is supported by the fact that the maximum values of these quantities are the most important ones for design. These results are presented in graphical, rather than in tabular form. The results of uniformly distributed load all over the plate and of the concentrated load at the center of the plate are given separately.

It should be noted that, in all the time history plots, a positive sign shows downward displacement and a negative sign shows upward displacement.

Uniformly distributed load case. The time histories of the center displacements for 10 m × 10 m and 10 m × 20 m plates when $H = 5$ m are presented in Figure 2. As seen from Figures 2(a) and 2(b), the center displacements of the 10 m × 10 m and 10 m × 20 m plates for $H = 5$ m reach their absolute maximum values of 10·2 mm at 3·08 s, and of 12·8 mm at 2·01 s, respectively.

As expected in a static sense, the maximum displacement of a 10 m × 20 m plate is larger than that of 10 m × 10 m plate, and the maximum displacement increases with increasing aspect ratio. Figures 2(a) and 2(b) indicate that the time histories of the center displacements of the plates differ from each other depending on the dynamic characteristics of the system. These figures show that the vibration periods of the center displacements are becoming larger with increasing aspect ratio for a fixed subsoil depth. This is expected because increasing the aspect ratio and/or the subsoil depth make the system more flexible when one side of the plate is kept constant as in this study. These figures also show that the plates vibrate just below the initial level.

The absolute maximum displacements of the plates are given in Figures 3 and 4 for different subsoil depths and aspect ratios, and for different H/ly ratios, respectively. Several general trends illustrated in Figures 3 and 4 are instructive. These trends seen from these figures are as follows.

The maximum displacement increases as the subsoil depth and/or the aspect ratio increase.

The subsoil depth has stronger influence on the maximum displacement than the aspect ratio for smaller values of subsoil depth, but the aspect ratio has stronger influence on the maximum displacement than the subsoil depth for the larger values of subsoil depth.

The maximum displacement decreases as the H/ly ratio increases for any values of the subsoil depth. This decrease is larger for smaller values of the

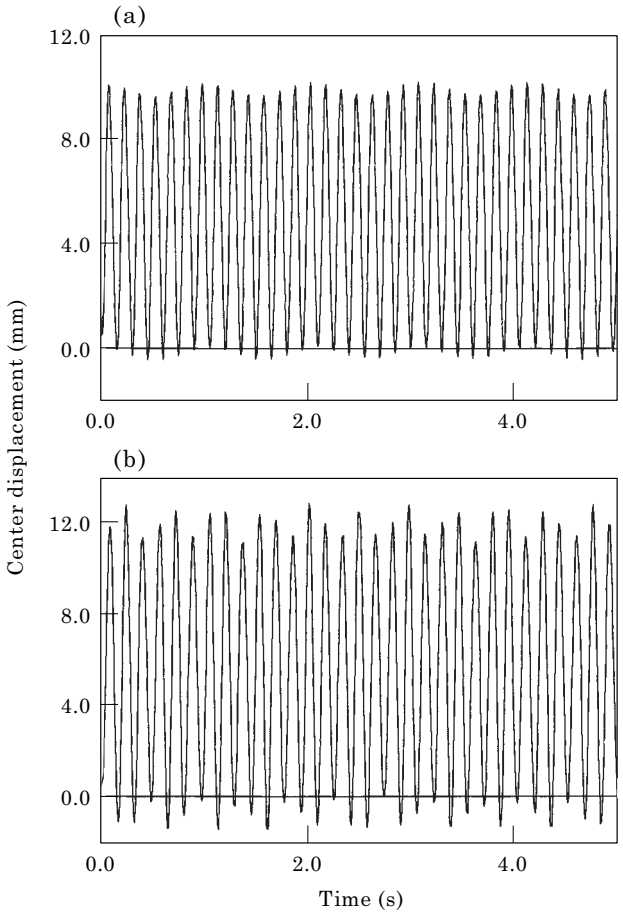

Figure 2. The time history of the center displacement of the plate subjected to uniformly distributed load (a) for $H = 5$ m and $ly = 10$ m; (b) for $H = 5$ m and $ly = 20$ m.

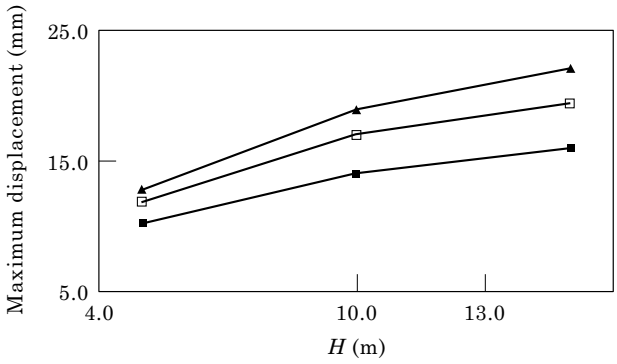

Figure 3. The maximum displacement of the plate subjected to the uniformly distributed load for different subsoil depths and aspect ratios. Key for l_y/l_x values: —■—, 1·0; —□—, 1·5; —▲—, 2·0.

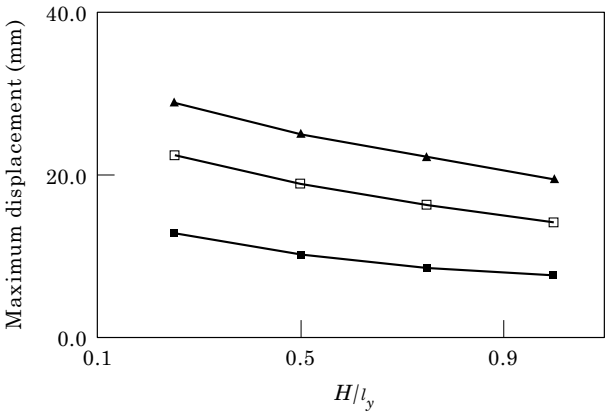

Figure 4. The maximum displacement of the plate subjected to the uniformly distributed load for different H/ly ratios and subsoil depths. Key for H values: —■—, 5 m; —□—, 10 m; —▲—, 15 m.

subsoil depth than for larger values of the subsoil depth because the maximum displacement tends to level off with increasing H/ly ratio. This behaviour is understandable in that a plate on elastic foundations with a larger subsoil depth becomes more flexible and thus less resistant to the load in a static sense.

The maximum displacement increases as the subsoil depth increases for any values of H/ly.

The deflected shapes of the 10 m × 10 m and 10 m × 20 m plates for $H = 15$ m for the time at which the maximum displacement occurs are given in Figure 5. As expected in a static sense, the center displacement of the plate with smaller subsoil depth and aspect ratios is smaller than that of the plate with larger subsoil depth and aspect ratio. The deflected shapes of the other plates considered are not presented since they are similar to the ones given here.

Concentrated load case. The time histories of the center displacements for 10 m × 10 m and 10 m × 20 m plates when $H = 5$ m are presented in Figure 6. As seen from Figures 6(a) and 6(b), the center displacements of the 10 m × 10 m and 10 m × 20 m plates for $H = 5$ m reach their absolute maximum values of 6·6 mm at 6·609 s, and of 5·8 mm at 5·482 s, respectively.

As in the case of uniformly distributed load, Figures 6(a) and 6(b) indicate that the time histories of the center displacements of the plate differ from each

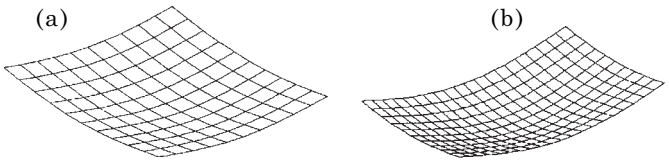

Figure 5. The deflected shape of the plate subjected to uniformly distributed load for different aspect ratios ($H = 15$ m). ly/lx values: (a) 1; (b) 2.

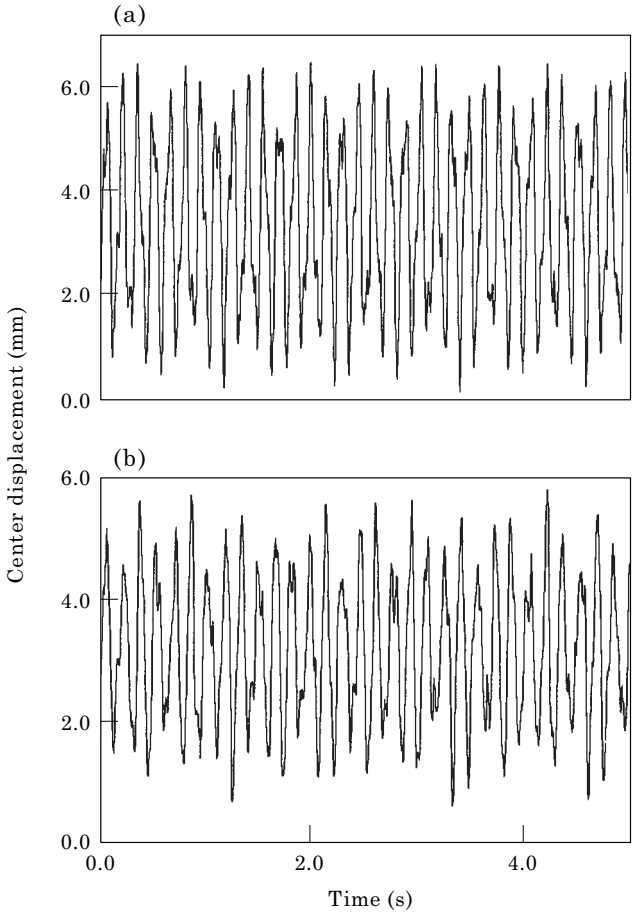

Figure 6. The time history of the center displacement of the plate subjected to concentrated load at the center (a) for $H = 5$ m and $ly = 10$ m; (b) for $H = 5$ m and $ly = 20$ m.

other depending on the characteristics of the plate–soil system, but in contrast to uniformly distributed load case, the center displacement is getting smaller with increasing aspect ratio for any values of subsoil depth.

It is seen from these figures that the vibration period of the center displacement is getting larger with increasing aspect ratio and/or subsoil depth, and that all of the plates considered always vibrate below the initial level, so that the plate edges have upward displacement as in the case of a beam subjected to concentrated load at mid-span [14].

The maximum displacement for different subsoil depths and aspect ratios are given in Figure 7. In this figure, the bottom part shows the upward displacements, and the top part shows the downward displacements. The curves of this figure are rather irregular in contrast to those of the plate subjected to the uniformly distributed load. The trends illustrated in this figure are as follows:

The maximum displacement increases with increasing subsoil depth for any values of ly/lx, except that upward displacement decreases when it is increased from 5 m to 10 m for $ly/lx = 1{\cdot}5$.

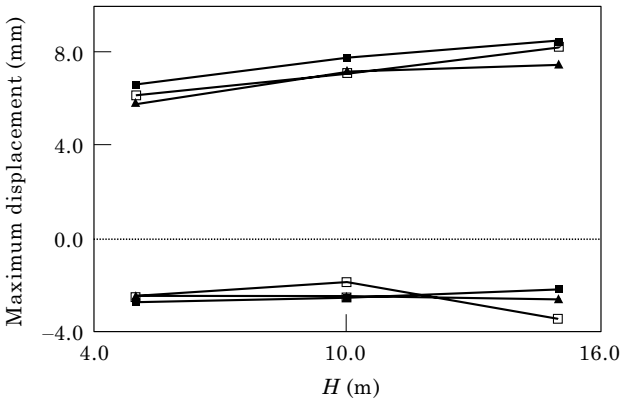

Figure 7. The maximum displacement of the plate subjected to concentrated load at the center for different subsoil depths and aspect ratios. Key as for Figure 3.

The maximum downward displacement generally decreases as the aspect ratio increases for any values of subsoil depth. This is not expected in a static sense, but the maximum displacement changes depending on the dynamic characteristics of the plate–soil system.

The effect of the subsoil depth on the maximum displacement is generally larger than that of the aspect ratio.

The deflected shapes of the 10 m × 10 m and 10 m × 20 m plates for $H = 5$ m and 15 m for the time at which the maximum displacement occurs are given in Figure 8. The deflected shapes of the other plates considered are not presented since they are similar to the ones given here.

Dynamic displacement of a plate resting on elastic foundations changes depending on the dynamic characteristics of the plate–soil system, so that, in contrast to the case of uniformly distributed load, the maximum displacement of the 10 m × 10 m plate for $H = 5$ m is larger than that of the 10 m × 20 m plate for the same subsoil depth.

It should be noted that the results obtained by using the consistent Vlasov model are not compared with the results of the Winkler model, which is simpler, because the stiffness parameter, k, which has a constant value in the Winkler model at all time increments, takes different values in the consistent Vlasov model at each time increment.

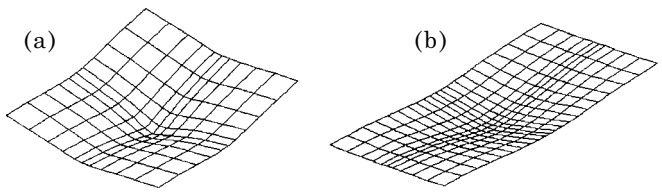

Figure 8. The deflected shape of the plate subjected to concentrated load at the center for different aspect ratios ($H = 15$ m). ly/lx values: (a) 1; (b) 2.

TABLE 1

The maximum and minimum γ values for different subsoil depths and aspect ratios

		γ_{min}		γ_{max}	
H (m)	ly/lx	*UDL*	*CL*	*UDL*	*CL*
5	1·00	0·81	0·79	2·56	6·28
	1·50	0·71	0·45	2·44	2·42
	2·00	0·66	0·40	2·22	2·22
10	1·00	1·24	1·22	5·70	13·93
	1·33	1·13	–	4·50	–
	1·50	1·10	0·74	5·55	5·42
	2·00	1·02	0·64	4·45	4·96
	4·00	0·90	–	2·48	–
15	1·00	1·60	1·57	7·16	22·25
	1·50	1·41	0·95	6·03	8·77
	2·00	1·30	0·83	6·60	8·01
	3·00	1·18	–	4·73	–
	6·00	1·07	–	3·43	–

The maximum and minimum values of the γ parameter obtained at each run for different subsoil depths and aspect ratios are presented in Table 1. As seen from this table, the values of γ generally increase with increasing subsoil depth for any values of the aspect ratio, and generally decrease with increasing aspect ratio for any values of the subsoil depth. This result agrees with the results obtained in references [8, 13]. As the value of γ increases, a mode shape, ϕ, defining the variation of displacement in the vertical direction [16] represents a rapidly dissipating displacement, which is typical for large values of H. When the value of γ approaches zero, the function ϕ yields a linear variation of displacements from top to bottom [8]. It should be noted that most of the values of γ obtained at each time increment are close to the minimum γ for all values of the subsoil depths and very large γ values such as 13·93 and 22·25 for the concentrated load are seen at a few time increments for all runs made.

If a plate resting on elastic foundations is subjected to the external load, it is not that difficult to talk about the effects of the subsoil depth and the aspect ratio on the response, because, in contrast to the beam resting on elastic foundations subjected to the vertical component of an earthquake [13], the curves are rather regular. The curves presented herein can help the designer to anticipate the effects of the subsoil depth and the aspect ratio on the maximum displacement of a plate resting on elastic foundations.

4. CONCLUSIONS

The consistent Vlasov model has been applied effectively to the dynamic analysis of plates resting on elastic foundations subjected to the external loads. Two soil parameters are iteratively calculated in terms of the parameter, γ, which

controls the decay of the stress distribution within the foundation. In addition, the following conclusions can be drawn from the results obtained in this study.

The maximum displacement generally increases as the subsoil depth and/or the aspect ratio increase for both loading cases.

The maximum displacement decreases with increasing H/ly ratio for any values of the subsoil depth for the uniformly distributed loading case.

The maximum displacement increases as the subsoil depth increases for any values of H/ly ratios for the uniformly distributed loading case.

In general, the effect of the change in the subsoil depth on the maximum displacement is larger than that of the change in the aspect ratio for both loading cases.

REFERENCES

1. M. Hetenyi 1961 *Beams on Elastic Foundations*. An Arbor, MI: The Michigan Press.
2. C. V. G. Vallabhan and Y. C. Das 1988 *ASCE, Journal of Engineering Mechanics* **114**, 2072–2082. Parametric study of beams on elastic foundations.
3. Z. Ding 1993 *Computers and Structures* **47**, 83–90. A general solution to vibrations of beams on variable Winkler elastic foundations.
4. J. Clastornik, M. Eisenberger, D. Z. Yankelevsky and M. A. Adin 1986 *ASME, Journal of Applied Mechanics*, **53**, 925–928. Beams on variable Winkler elastic foundation.
5. M. Eisenberger, D. Z. Yankelevsky and J. Clastornik 1986 *Computers and Structures* **24**, 135–140. Stability of beams on elastic foundations.
6. M. Eisenberger and J. Clastornik 1987 *Journal of Sound and Vibration* **115**, 233–241. Vibrations and buckling of a beam on Winkler elastic foundation.
7. M. A. De Rosa 1989 *Earthquake Engineering and Structural Dynamics* **18**, 377–388. Stability and dynamics of beams on Winkler elastic foundation.
8. C. V. G. Vallabhan, W. T. Straughan and Y. C. Das 1991 *ASCE, Journal of Engineering Mechanics* **117**, 2830–2844. A refined model for analysis of plates on elastic foundations.
9. C. Franciosi and A. Masi 1993 *Computers and Structures* **47**, 419–426. Free vibrations of foundation beams on two-parameter elastic soil.
10. M. A. De Rosa 1993 *Computers and Structures* **49**, 341–349. Stability and dynamics of two-parameter foundation beams.
11. T. Yokoyama 1996 *Computers and Structures* **61**, 995–1007. Vibration analysis of Timoshenko beam-columns on two-parameter elastic foundations.
12. V. Z. Vlasov and N. N. Leont'ev 1966 *Israel Program for Scientific Translations, Jerusalem, Israel*. Beams, plates and shells on elastic foundations.
13. Y. Ayvaz and A. Daloğlu 1997 *Journal of Sound and Vibration* **200**, 315–325. Earthquake analysis of beams resting on elastic foundations by using a modified Vlasov model.
14. A. Daloğlu and Y. Ayvaz 1996 *Proceedings of the Second International Conference in Civil Engineering on Computer Applications, Research and Practice* **3**, 901–907. Vibration analysis of beams on elastic foundation using modified Vlasov model.
15. V. Kolar and I. Nemec 1989 *Modelling of Soil–Structure Interaction*. Amsterdam: Elsevier.
16. Y. Ayvaz, A. Daloğlu and A. Doğangün 1998 *Journal of Sound and Vibration* **212**, 499–509. Application of modified Vlasov model to earthquake analysis of plates resting on elastic foundation.

17. A. TURHAN 1992 *Ph.D. Thesis, The Graduate School of Texas Tech University, Lubbock, Texas*. A consistent Vlasov model for the analysis of plates on elastic foundations using the finite element model.
18. J. L. HUMAR 1990 *Dynamics of Structures*. Englewood Cliffs, NJ: Prentice-Hall.